



Virtual non-enhanced dual-energy computed tomography reconstruction: a candidate to replace true non-enhanced computed tomography scans in the setting of suspected liver alveolar echinococcosis

Mecit Kantarcı 
Sonay Aydın 
Aşegül Kahraman 
Hayri Oğul 
Barış İrgül 
Akin Levent 

From the Department of Radiology (M.K., H.O.), Atatürk University, Faculty of Medicine, Erzurum, Turkey; Department of Radiology (S.A., B.I. ✉ barisirgul@gmail.com, A.L.), Erzincan Binali Yıldırım University, Faculty of Medicine, Erzincan, Turkey; Department of Radiology (A.K.), İnönü University, Faculty of Medicine, Malatya, Turkey.

Received 31 July 2022; revision requested 05 October 2022; last revision received 11 March 2023; accepted 26 March 2023.



Epub: 12.04.2023

Publication date: 07.11.2023

DOI: 10.4274/dir.2023.221806

PURPOSE

When a suspected hepatic alveolar echinococcosis (AE) lesion is detected on a contrast enhanced computed tomography (CT) scan, an additional triphasic or non-enhanced CT scan is required to determine the presence of calcification and enhancement. As a result, imaging costs and exposure to ionizing radiation will increase. We can create a non-enhanced series from routine contrast-enhanced images using dual-energy CT (DECT) and virtual non-enhanced (VNE) images. This study's objective is to assess virtual non-enhanced DECT reconstruction as a potential diagnostic tool for hepatic AE.

METHODS

Triphasic CT scans and a routine dual energy venous phase were acquired using a third-generation DECT system. A commercially available software package was used to generate VNE images. Individual evaluations were conducted by two radiologists.

RESULTS

The study population consisted of 100 patients (30 AE, 70 other solid liver masses). All AE cases were diagnosed [no false positives/negatives, 95% confidence interval (CI) sensitivity: 91.3%–100%; 95% CI specificity: 95.3%–100%]. Interrater agreement was $k = 0.79$. In total, 33 (33.00%) of the patients had AE, which was detected using both true non-enhanced (TNE) and VNE images. The mean dose-length product of a standard triphasic CT was significantly higher than biphasic dual-energy VNE images.

CONCLUSION

In terms of diagnostic confidence, VNE images are comparable with actual non-enhanced imaging when evaluating hepatic AE. Further, VNE images could replace TNE images with a substantial radiation dose reduction. Advances in knowledge: hepatic cystic echinococcosis and AE are serious and severe diseases with high fatality rates and a poor prognosis if managed incorrectly, especially AE. Moreover, VNE images produce equal diagnostic confidence to TNE images for assessing liver AE, with a significant reduction in radiation dose.

KEYWORDS

DECT, virtual non-enhanced, alveolar echinococcosis, DLP, radiation

Echinococcosis is a largely global zoonotic illness caused by Echinococcus-genus family cestodes. Both *Echinococcus granulosus* and *Echinococcus multilocularis* (*E. granulosus*) are medically and publicly significant because they cause cystic echinococcosis (CE) and alveolar echinococcosis (AE), respectively. Both hepatic CE and AE are severe disorders with significant mortality rates and a poor prognosis if improperly treated, especially AE. The prev-

You may cite this article as: Kantarcı M, Aydın S, Kahraman A, Oğul H, İrgül B, Levent A. Virtual non-enhanced dual-energy computed tomography reconstruction: a candidate to replace true non-enhanced computed tomography scans in the setting of suspected liver alveolar echinococcosis. *Diagn Interv Radiol.* 2023;29(6):736-740.

absence of AE is highest in the northern hemisphere, specifically in Central Europe, Turkey, Russia, Japan, Alaska, North America, and China. Approximately 18,000 new cases of AE are reported annually across the globe.¹⁻³

Untreated hepatic AE is invariably fatal, and the therapeutic response is difficult to evaluate once detected. Importantly, radiologists must guarantee rapid referral to experts and imaging follow-up; however, due to the variability of AE imaging findings, initial misinterpretation is prevalent, particularly in non-endemic regions. Imaging methods such as ultrasonography, computed tomography (CT), and magnetic resonance imaging work well together to aid in the diagnosis, morphology, and treatment choices of AE lesions.^{4,5} Typical hepatic AE calcifications are best seen on non-enhanced CT images. Moreover, demonstrating the absence of enhancement in AE lesions is a critical diagnostic feature for differentiating AE from hepatic tumors.

When a suspected hepatic AE lesion is detected on a contrast-enhanced CT scan, an additional triphasic or non-enhanced CT scan is required to determine the presence of calcification and enhancement. As a result, imaging costs and exposure to ionizing radiation will increase. It is possible to create a non-enhanced series from routine contrast-enhanced images using dual energy CT (DECT) and virtual non-enhanced (VNE) images with a significantly reduced radiation dose.⁶ Previously, DECT was evaluated for the diagnosis of hepatic AE. Previous studies primarily emphasized DECT's ability to define the micro-perfusion status of the periparasitic granulomatous reaction and the consistency of DECT findings with positron emission tomography-CT results.^{7,8} Consequently, the objective of this study is to investigate the diagnostic potential of VNE DECT reconstruction for hepatic AE.

Main points

- Virtual non-enhanced (VNE) images can be used effectively in place of true non-enhanced images to diagnose hepatic alveolar echinococcosis (AE).
- Using VNE images reduces exposure to ionizing radiation.
- Despite a considerable drop in noise, sharpness, and image quality in VNE, both non-enhanced scans detect liver AE comparably.

Methods

Study population

A database search was conducted using electronic archives for patients who were imaged for liver mass characterization between December 2016 and December 2021 for this retrospective cohort study. Approval from the Ethics Committee was acquired (Erzincan Binali Yıldırım University Clinical Research Ethics Committee, EBYU-KAEK-2022- 01.003-28). Patients were included if they had the following: I) liver mass; and II) a multiphase/triphasic CT exam. Exclusion criteria included the following: I) mono- or biphasic CT examinations; and II) multiphase CT examinations without the use of dual energy. The study included only those patients with an AE diagnosis. To avoid selection bias and to create a more diverse study group, patients with non-AE liver masses (twice the number of patients with an AE diagnosis) were also randomly selected and included in the study group. One author formed the study group independently of the authors who evaluated the images.

Imaging protocol: triphasic CT scans with ADMIRE strength 2 (advanced modeled iterative reconstruction) and routine dual energy venous phase were obtained via a third-generation dual-source dual-energy 2x192 slice-CT system (Siemens Somatom Force, Siemens Healthcare, Erlangen, Germany).

True non-enhanced (TNE) images scan parameters were as follows: the reference tube voltage was 120 kVp, the effective tube current was adapted to the patient's body mass, the quality reference mAs was 147 QrefmAs, the dose modulation was CARE dose 4D, the CARE kV was turned on, the slice thickness was 3 mm, and the reconstruction kernel was Br40. For contrast-enhanced phases, the following scan parameters were used: reference tube voltage: 100 kVp, effective tube current: patient body mass adjusted, quality reference mAs: 190 QrefmAs, dose modulation: CARE dose 4D, CARE kV: on, slice thickness: 3 mm, reconstruction kernel: Bf40 (venous), and Br40 (venous) (arterial).

Iohexol was injected at a flow rate of 4 mL/s and adapted to the patients' body weight (1 mL/kg body weight), followed by a saline flush. TNE images were acquired first, followed by arterial and venous phase images 20 and 80 seconds after contrast agent injection, respectively.

VNE image calculation

A commercially available software package (SyngoVia VB20A, Siemens Healthcare, Forchheim, Germany) was used to generate VNE datasets (Figures 1, 2). Reconstruction was performed axially with the same slice thickness of 3 mm as for TNE images to obtain identical images.

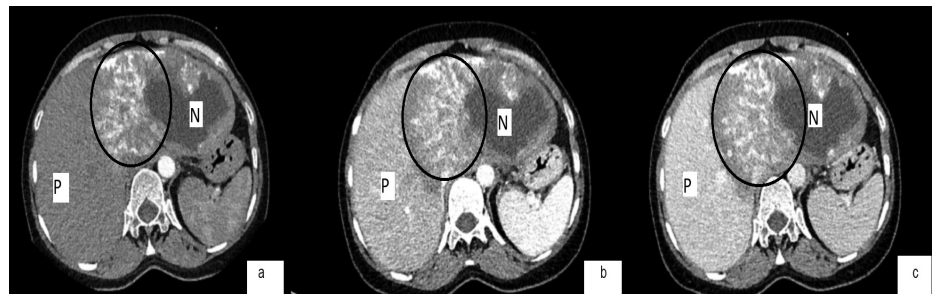


Figure 1. Arterial (a), portal venous (b), hepatic venous (c), axial computed tomography images of a hepatic alveolar echinococcosis with typical calcification pattern (circle), necrotic areas (N), and irregular contours with normal parenchyma (P).

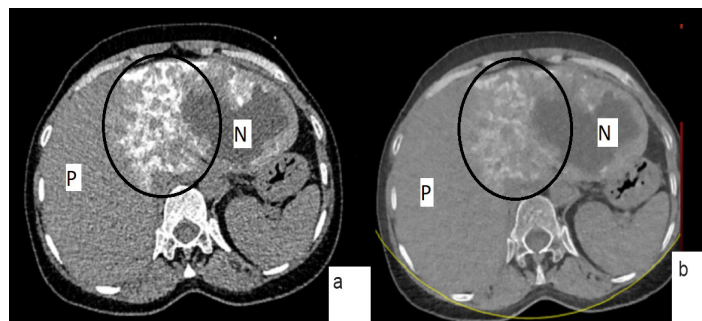


Figure 2. True non-enhanced (a) and virtual non-enhanced (b) images of a hepatic alveolar echinococcosis with typical calcification pattern (circle), necrotic areas (N), and irregular contours with normal parenchyma (P).

Assessment of image quality

Two radiologists with 8 and 25 years' experience in abdominal imaging evaluated the image quality independently. If two independent readers disagreed on the diagnosis of an adverse event, a consensus reading was conducted. To reduce recall bias, all cases were evaluated randomly and anonymously in two sessions separated by eight weeks. The following datasets were provided by the studying supervisor for these sessions: 1. venous, arterial, and VNE images; and 2. venous, arterial, and TNE images. The various datasets were distributed randomly and blindly to both readers during the initial session. During the second session, the non-enhanced phase of the dataset was evaluated for the first time. Both readers scored TNE and VNE images on a 5-point Likert scale for overall image quality, noise, artefacts, and sharpness (5 being the best outcome of the evaluated category and 1 being the worst).

Diagnostic performance

The researchers were asked to make a diagnosis of AE or non-AE based on the presence and absence of calcification enhancement. With TNE or VNE images in conjunction with the arterial and venous phases and a 5-point Likert scale, diagnostic confidence in the presence or absence of AE was evaluated

(1 not confident, 2 low confidence, 3 moderate confidence, 4 confident, and 5 high confidence).

Radiation dose

To evaluate the reduction in X-ray exposure, the total dose-length product (DLP) of all three phases (TNE, arterial, and venous) and the total DLP of only the arterial and venous phases were determined for each patient.

Statistical analysis

SPSS was used to conduct the statistical analysis (IBM SPSS Statistics 24). To evaluate the normally distributed data, the Kolmogorov-Smirnov test was utilized. Continuous variables with normal distribution [age, Hounsfield units (HU) values, and DLP values] were represented by their mean and standard deviation, numerical variables with non-normal distribution were given as the median (min-max) (image quality, noise, sharpness, diagnostic confidence, and artefact elimination scores), while the categorical variables (gender) were represented by their percentage (%). The Wilcoxon paired test was used to compare the overall image quality, noise, sharpness, artefact elimination, and diagnostic confidence. Sensitivity and specificity were calculated using cross tabulation

and expressed in percent (%), including the 95% confidence interval (CI). The paired t-test was utilized to determine the DLP's significance. Cohen's kappa coefficient was used to determine the interrater agreement for the image quality, noise, sharpness, artefact elimination, and diagnostic confidence. Kappa values (k) of agreement were defined as poor between 0.01 and 0.20, fair between 0.21 and 0.40, moderate between 0.41 and 0.60, substantial between 0.61 and 0.80, and nearly perfect between 0.81 and 1.00.⁹

The level of significance was accepted as α : 0.05.

Results

The study population consisted of 100 patients (30 AE, 70 other solid liver masses). The mean age of the population was 56.23 ± 11.72 years (min - max, 31-78 years). A total of 63 (63%) of the patients were male and 37 (37%) were female (Table 1).

Image quality

A comparison of the TNE and VNE image quality revealed statistically significant variations ($P < 0.001$). In terms of the overall image quality, noise, and sharpness, TNE images outperformed VNE images, whereas VNE images exceeded TNE images in terms of artefact elimination. Interrater agreement was substantial for the aforementioned categories (k: 0.63-0.75) (Figure 3) (Tables 2, 3).

Diagnostic performance

Both non-enhanced series had excellent diagnostic confidence, with TNE images indicating statistically significant superiority ($P = 0.030$). Significant interrater agreement was observed (k: 0.79, $P = 0.006$) (Tables 4, 5). In total, 33% of the enrolled individuals had adverse events that were recognized using both TNE and VNE images. All AE cases were detected (no false positives or negatives), resulting in a sensitivity and specificity of 100% (95% CI sensitivity: 91.3%-100%; 95% CI specificity: 95.3%-100%). Perfect agreement existed between the researchers regarding the detection of AE (k: 1, $P = 0.001$).

The ROIs positioned in the solid portions of the lesions had a substantially higher mean HU values for TNE than VNE images ($P = 0.03$), and the measurement error was 21.1 ± 10.30 (45.3 ± 11.8 vs. 61.7 ± 10.4 HU).

Radiation dose

Biphasic dual-energy CT with VNE images had a mean DLP of 1613.8 ± 421.7 mGy cm,

Table 1. Characteristics of the study population

Characteristic	Value
Number of patients	100
Distribution of the lesions	30 alveolar echinococcosis, 70 other solid liver masses
Mean age	56.23 ± 11.72 years
Number of males and females	M: 63 (63%), F: 37 (37%)

M, male; F, female.

Table 2. Median quality parameters

Image quality parameters	Median score		P value
	TNE n = 100	VNE n = 100	
Overall image quality	4 (1-5)	3 (1-4)	0.001
Noise	4 (1-5)	2 (1-5)	0.001
Sharpness	4 (1-5)	2 (2-5)	0.001
Artefact elimination	2 (2-5)	4 (1-4)	0.001

TNE, true non-enhanced; VNE, virtual non-enhanced.

Table 3. Interobserver reliability data for quality parameters

Image quality parameters	Kappa value (k)	P value
Overall image quality	0.63	0.004
Noise	0.69	0.010
Sharpness	0.75	0.020
Artefact elimination	0.71	0.008

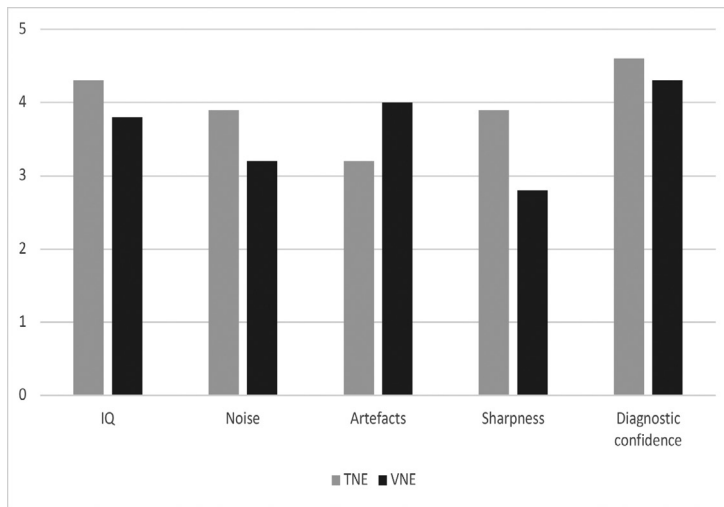


Figure 3. Subjective image analysis and diagnostic confidence as rated by the primary reader for TNE and VNE. The data are expressed as the mean (range). IQ, image quality; TNE, true non-enhanced; VNE, virtual non-enhanced.

Diagnostic performance	Median score		P value
	TNE n = 100	VNE n = 100	
Diagnostic confidence according to presence of calcification	5 (3–5)	4 (2–5)	0.030

TNE, true non-enhanced; VNE, virtual non-enhanced.

Diagnostic performance	Kappa value (k)	P value
Diagnostic confidence according to presence of calcification	0.79	0.006

indicating a significant reduction in radiation exposure in comparison with standard triphasic CT, where the DLP was $1,985.3 \pm 343$ mGy cm ($P < 0.001$).

Discussion

The objective of this investigation was to compare VNE DECT reconstruction with actual non-enhanced CT scans for the diagnosis of hepatic AE. The authors demonstrated that VNE images can be used effectively in place of TNE images to diagnose hepatic AE. Additionally, using VNE images reduces exposure to ionizing radiation.

Despite a considerable drop in noise, sharpness, and image quality in VNE, this study revealed that both non-enhanced scans detect liver AE comparably. The authors were able to demonstrate that compared with TNE images, VNE images significantly reduced artefacts.

As a result of these findings, the authors believe that the genuine non-enhanced phase can be substituted with VNE images,

which enables a substantial reduction in radiation dose. If an elimination can be succeeded in artefacts of VNE images, this method may provide even more information than TNE images. Although VNE attenuation is believed to be comparable with that of TNE images, the literature has already showed discrepancies between 5 and 15 HU.^{10–12} Toepker et al.¹³ found a mean difference of -3.6 ± 8.3 HU between the non-enhanced and enhanced datasets. Consequently, comparable attenuation values are observed between TNE and VNE images.¹³ Additional studies demonstrated that organ-specific attenuation values exist. Renal parenchyma, liver, and aorta all exhibited statistically significant variations; however, spleen and fat attenuation did not.¹⁴ We believe that by achieving perfect interrater agreement between VNE and TNE images, we can overcome the limitations imposed by HU differences.

Sun et al.¹⁵ examined dual-source DECT versus TNE images in 112 suspected gastrointestinal bleeding cases and stated that VNE had lower image quality and noise levels

than TNE. These results contradict those of this study, which demonstrated a significant change in the image quality and an increase in noise levels in VNE images.¹⁵ Nonetheless, the findings were consistent regarding the use of VNE images.

Overall, CT was commonly emphasized as the best imaging modality to diagnose hepatic AE, as it enables anatomic and morphologic characterization of lesions and provides the most accurate representation of the calcification pattern. Along with the calcification pattern, enhancement characteristics are critical, particularly when differentiating tumoral lesions. After administration of an intravenous contrast medium, no significant enhancement was observed within the hepatic AE lesion; however, the fibroinflammatory component surrounding the parasitic tissue may have been slightly enhanced in the delayed phase.^{3,16} The primary issue with CT examinations in clinical practice, particularly triphasic CT examinations, is the exposure to high doses of radiation.^{8,16}

Although the role of DECT in liver AE has been studied recently, previous research has focused on the perfusion characteristics of hepatic AE lesions, the use of perfusion differences to differentiate AE from hepatic malignancies, the role of perfusion imaging in monitoring treatment response, and the presence of periparasitic granulomatous tissue as increased perfusion.^{16,17} There are no prior studies that the authors are aware of that examines the diagnostic success of VNE images in the diagnosis of liver AE.

Other abdominal pathologies have been studied to determine the diagnostic success of VNE imaging. When comparing the detection rates of diseases in VNE and TNE images in 15 patients with “acute abdominal pain”, Im et al.¹⁸ discovered that the detection rates and visual quality of the unmodified photographs were practically comparable. Flors et al.¹⁹ observed equivalent results while evaluating the presence of endoleak in 48 patients following endovascular aortic repair (EVAR). By comparing a standard triphasic procedure with actual non-enhanced images and a monophasic and biphasic protocol to VNE images, they concluded that VNE images plus a delayed phase can be employed in place of the usual triphasic protocol for post-EVAR CT examinations.¹⁹

This study is not without limitations. First, the retrospective nature of the study may have introduced a selection bias. However, the study included randomly selected patients to ensure a representative sample. Sec-

ond, due to the transferable clinical setting, image quality was only subjectively assessed. Third, the authors simulated non-enhanced images using a single piece of software without comparing it with other pieces of software. As a result, more advanced software may exist. As in previous studies, VNE images had lower HU values than TNE images. When compared with enhanced images, it is possible that this situation will be misinterpreted as contrast enhancement. However, because this HU change occurs in normal liver parenchyma as well, comparing the HU values of normal parenchyma and the lesion together will resolve the previously mentioned potential confusion. To confirm these preliminary results, a larger cohort or external cross-validation is required.

In conclusion, the findings show that VNE images produce equal diagnostic confidence and perfect agreement with TNE images for assessing liver AE. This implies that VNE images could replace TNE images, resulting in a significant reduction in the radiation dose.

Conflict of interest disclosure

The authors declared no conflicts of interest.

References

- Romig T, Deplazes P, Jenkins D, et al. Ecology and life cycle patterns of *Echinococcus* species. *Adv Parasitol.* 2017;95:213-314. [\[CrossRef\]](#)
- Guo H, Liu W, Wang J, Xing Y. Extrahepatic alveolar echinococcus on multi-slice computed tomography and magnetic resonance imaging. *Sci Rep.* 2021;11(1):9409. [\[CrossRef\]](#)
- Kantarci M, Bayraktutan U, Karabulut N, et al. Alveolar Echinococcosis: spectrum of findings at cross-sectional imaging. *Radiographics.* 2012;32(7):2053-2070. [\[CrossRef\]](#)
- Sade R, Kantarci M, Ogul H, Gundogdu B, Aydinli B. Differentiation between hepatic alveolar echinococcosis and primary hepatic malignancy with diffusion-weighted magnetic resonance imaging. *Diagn Interv Imaging.* 2018;99(3):169-177. [\[CrossRef\]](#)
- Chouhan MD, Wiley E, Chiodini PL, Amin Z. Hepatic alveolar hydatid disease (*Echinococcus multilocularis*), a mimic of liver malignancy: a review for the radiologist in non-endemic areas. *Clin Radiol.* 2019;74(4):247-256. [\[CrossRef\]](#)
- Walter SS, Schneeweiß S, Maurer M, et al. Virtual non-enhanced dual-energy CT reconstruction may replace true non-enhanced CT scans in the setting of suspected active hemorrhage. *Eur J Radiol.* 2018;109:218-222. [\[CrossRef\]](#)
- Sade R, Kantarci M, Genc B, Ogul H, Gundogdu B, Yilmaz O. Computed tomography perfusion imaging for the diagnosis of hepatic alveolar Echinococcosis. *Eurasian J Med.* 2018;50(1):1-5. [\[CrossRef\]](#)
- Liu W, Delabrousse É, Blagosklonov O, et al. Innovation in hepatic alveolar echinococcosis imaging: best use of old tools, and necessary evaluation of new ones. *Parasite.* 2014;21:74. [\[CrossRef\]](#)
- McHugh ML. Interrater reliability: the kappa statistic. *Biochem Med (Zagreb).* 2012;22(3):276-282. [\[CrossRef\]](#)
- Bonatti M, Lombardo F, Zamboni GA, Pernter P, Pozzi Mucelli R, Bonatti G. Dual-energy CT of the brain: comparison between DECT angiography-derived virtual unenhanced images and true unenhanced images in the detection of intracranial haemorrhage. *Eur Radiol.* 2017;27(7):2690-2697. [\[CrossRef\]](#)
- Kaufmann S, Sauter A, Spira D, et al. Tin-filter enhanced dual-energy-CT: image quality and accuracy of CT numbers in virtual noncontrast imaging. *Acad Radiol.* 2013;20(5):596-603. [\[CrossRef\]](#)
- Kaza RK, Raff EA, Davenport MS, Khalatbari S. Variability of CT attenuation measurements in virtual unenhanced images generated using multiterminal decomposition from fast kilovoltage-switching dual-energy CT. *Acad Radiol.* 2017;24(3):365-372.
- Toepker M, Moritz T, Krauss B, et al. Virtual non-contrast in second-generation, dual-energy computed tomography: reliability of attenuation values. *Eur J Radiol.* 2012;81(3):e398-e405. [\[CrossRef\]](#)
- Sahni VA, Shinagare AB, Silverman SG. Virtual unenhanced CT images acquired from dual-energy CT urography: accuracy of attenuation values and variation with contrast material phase. *Clin Radiol.* 2013;68(3):264-271. [\[CrossRef\]](#)
- Sun H, Hou XY, Xue HD, et al. Dual-source dual-energy CT angiography with virtual non-enhanced images and iodine map for active gastrointestinal bleeding: image quality, radiation dose and diagnostic performance. *Eur J Radiol.* 2015;84(5):884-891. [\[CrossRef\]](#)
- Bulakçı M, Kartal MG, Yılmaz S, et al. Multimodality imaging in diagnosis and management of alveolar echinococcosis: an update. *Diagn Interv Radiol.* 2016;22(3):247-256. [\[CrossRef\]](#)
- Oğul H, Kantarcı M, Genç B, et al. Perfusion CT imaging of the liver: review of clinical applications. *Diagn Interv Radiol.* 2014;20(5):379-389. [\[CrossRef\]](#)
- Im AL, Lee YH, Bang DH, Yoon KH, Park SH. Dual energy CT in patients with acute abdomen; is it possible for virtual non-enhanced images to replace true non-enhanced images? *Emerg Radiol.* 2013;20(6):475-483. [\[CrossRef\]](#)
- Flors L, Leiva-Salinas C, Norton PT, Patrie JT, Hagspiel KD. Endoleak detection after endovascular repair of thoracic aortic aneurysm using dual-source dual-energy CT: suitable scanning protocols and potential radiation dose reduction. *AJR Am J Roentgenol.* 2013;200(2):451-460. [\[CrossRef\]](#)